A HREEL investigation of adsorption and dissociation of NO on a Rh(110) surface

Cautero, G.; Astaldi, C.; Rudolf, P.; Kiskinova, M.; Rosei, R.

A HREEL investigation of adsorption and dissociation of NO on a Rh(110) surface

G. Cautero [a], C. Astaldi [b], P. Rudolf [b], M. Kiskinova [a,b] and R. Rosei [a,b,c]

[a] Sincrotrone Trieste, Padriciano 99, 34012 Trieste, Italy
[b] Laboratorio INFM-TASC, Padriciano 99, 34012 Trieste, Italy
[c] Dipartimento di Fisica, Univesita di Trieste, via A. Valerio 2, I-34127, Trieste, Italy

The adsorption and dissociation of NO on a Rh(110) surface in the temperature range from 100 to 300 K has been studied by means of high-resolution electron energy loss (HREEL) spectroscopy. At 100 K only one adsorption state of NO, assigned to bridge-bonded NO species, is observed at the whole NO coverage range. The N–O stretching frequency of this species increases from 1560 to 1710 cm^{-1} with increasing NO coverage. NO decomposition, which occurs readily at temperatures above 170 K has been studied for NO coverages less than 0.3 of the saturated NO coverage at 100 K. The HREELS data have shown that the fraction of NO molecules which undergo dissociation increases with increasing temperature and with decreasing initial NO coverage. For the highest NO coverages considered (0.3 of saturation at 100 K) all NO molecules decompose at 240 K. A variety of loss features are observed in the HREEL spectra after decomposition of different amounts of NO. These HREEL data are explained on the basis of comparison with the HREEL spectra measured for oxygen, nitrogen and mixed oxygen and nitrogen layers on Rh(110). It has been established that the variety of loss features observed after dissociation of NO is due to different oxygen states on the surface. The observed effect of the dissociation products on the N–O stretching frequencies have been discussed considering the factors that can account for the blue-shifts observed in the presence of electronegative surface modifiers.

1. Introduction

The interaction of NO with single-crystal metal surfaces attracts interest mainly because NO is one of the most toxic components in the automobile exhaust gases. Undoubtedly, fundamental understanding of the nature of NO adsorption bond, which exhibits a variety of possible configurations, is an important step in strengthening the theoretical basis in the search of effective metal catalysts for neutralization of NO. Since the neutralization process involves as an intermediate step NO dissociation, the dissociative propensity of the various adsorption configurations of NO on metal surfaces has been a subject of many investigations. A variety of NO bonding configurations have been observed. They are assigned to on-top and bridge linear [1–20], on-top and bridge bent [6,16,17], threefold [19] and side-on [20] bonding and the formation of (NO)$_2$ dimers [11].

Vibrational spectroscopy data have shown that the bridge bonding is the preferred adsorption configuration especially at low NO coverages [1–15]. NO adsorbed on various single crystal metal surfaces exhibits a different tendency towards dissociation. It retains its molecular form on Pt(111) [7–10], Pd(111) [12,27,28] and Pd(100) [11,14] surfaces independently on the adsorption temperature. Both molecular and dissociative adsorption occurs on Ni [16–18], Ru [1–4,19], Rh [13–15,20–26], Pt(100) [6], Ir [5,29,30], Re [31], Mo [32,33] and Ag(111) [34] surfaces. The dissociative propensity of NO varies with different metals and is substantially influenced by the substrate surface structure and the presence of defects [25].

Recently, several research groups focused on studies of NO adsorption and dissociation on Rh single-crystal surfaces [13–15,20–26]. The interest in NO/Rh systems is explained by the fact that

Rh is one of the most effective catalysts used in automobile converters [35]. The NO bonding configuration (adsorption site and bonding geometry) has been already studied on Rh(111) [13,22] and Rh(100) [20] surfaces. In the case of the NO/Rh(111) system there is certain disagreement in the reported vibrational data for what concerns the low-frequency region and at high NO coverages, the high-frequency region as well. The HREELS studies by Root et al. [13] have shown a single bridge-bonded NO state with NO molecular axis normal to the surface plane at all coverages. This species is characterized by a N–O stretching mode in the range of 1500–1600 cm^{-1} and a very weak Rh–NO band at ~ 360 cm^{-1} and undergoes dissociation at temperatures above 250 K. Kao et al. [22] reported a Rh–NO band at 435 cm^{-1} and an occurrence of extra features at 400, 485, 1515 and 1830 cm^{-1} after very large exposures of NO at 250 K. These features gain intensity at the expense of the initial losses at 435 and 1635 cm^{-1}. The new losses were assigned to occupation of bridge and on-top sites in a dense ordered layer. For NO adsorption on Rh(100) a highly inclined species, characterized by a stretching frequency of 920 cm^{-1}, were detected at low NO coverages and at temperatures lower than 140 K [20]. This NO species readily dissociates at temperatures above 140 K. A second bridge-bonded NO species on Rh(100), characterized by vibrational modes in the 1580–1678 cm^{-1} range, were observed at moderate and high coverages. This species exhibits a strong coverage dependence of its dissociation rate [20]. To our knowledge only one study on the adsorption of NO on Rh(110) at room temperature has been reported [26]. The TPD and XPS results in this study indicate that at room temperature the initial NO adsorption on Rh(110) is dissociative, followed by molecular NO adsorption at higher coverages.

The present HREELS study of NO adsorption on Rh(110) is carried out in the temperature range of 100–300 K. It addresses two aspects: (i) the bonding configuration of molecular NO at 100 K at various coverage, and (ii) the changes in the HREEL spectra as a result of NO decomposition. Since only below a certain NO coverage NO undergoes complete dissociation prior to des-

orption, the NO decomposition studies presented in this paper consider relatively low NO coverages. Special attention was paid to the identification of the adsorption state of the dissociation products O and N and their effect on the NO stretching frequencies at the NO coverages under investigation.

2. Experimental

The experiments were carried out in an UHV apparatus consisting of two chambers. The cleaning procedures, the characterization of the sample and the exposure to NO were performed in the preparation chamber. It contains an ion gun, facilities for LEED and Auger spectroscopy and leak valves for gas inlet. The second chamber is equipped with a Leybold ELS22 spectrometer, operating at a pressure of 4×10^{-11} mbar. The energy resolution achieved was usually ~ 5–6 meV (40–50 cm^{-1}). The HREEL spectra in the present study were taken using a primary energy of 1.7 eV. The incident angle of the electrons was 60° from the surface normal. Most of the spectra were measured in a specular geometry. A few experiments with electrons collected in a direction at 4, 10 and 16° off-specular also were performed. HREEL spectra were normalized to the integrated elastic peak intensity. The areas of the elastic and loss peaks were determined by the least-squares Gaussian fits.

The Rh single crystal was oriented within 1° of the [110] direction. It was mounted onto two tungsten wires which allowed direct resistive heating of the sample up to 1300 K. The temperature was measured using a chromel–alumel thermocouple which was forced into a narrow hole in the sample. The crystal was cleaned by repeated cycles of Ne bombardment, heating in 2×10^{-8} mbar oxygen at 1100 K and annealing to 1300 K until no contaminants were distinguished in the AES and HREEL spectra. The HREEL spectrum of a clean Rh(110) surface shows only a feature at ~ 160 cm^{-1} assigned to a Rh phonon. All HREEL measurements were carried out at a sample temperature of 100 K, i.e., after cooling down the sample provided a heat treatment had

been performed after adsorption of NO at 100 K. The heating temperatures used in the studies of dissociation of NO were in the range 180–240 K. The cooling time required to "freeze" the reaction at 100 K was of the order of a few seconds.

3. Results

3.1. NO adsorption at 100 K

Since no LEED patterns were detected during NO adsorption we had no reference point to determine the absolute NO coverage. That is why the coverage calibration was performed on the basis of the NO uptake curve taken by monitoring the increase of the integrated intensity of the N(KLL) Auger peak with increasing NO exposure at 100 K. The saturation NO coverage at 100 K, which was achieved at exposures of ~ 10 L (1 L $= 10^{-6}$ Torr s), was assigned as a relative coverage of $\theta = 1$. On this basis the NO coverages, θ_{NO}, obtained upon different NO exposures, are presented as a fraction of the saturated coverage at 100 K.

Fig. 1 shows a series of HREEL spectra of NO adsorbed on Rh(110) at 100 K. Adsorption results in an appearance of one N–O stretching mode which shifts from 1560 to 1710 cm^{-1} with increasing θ_{NO}. In the low-energy region NO induces initially a rather broad poorly resolved feature in

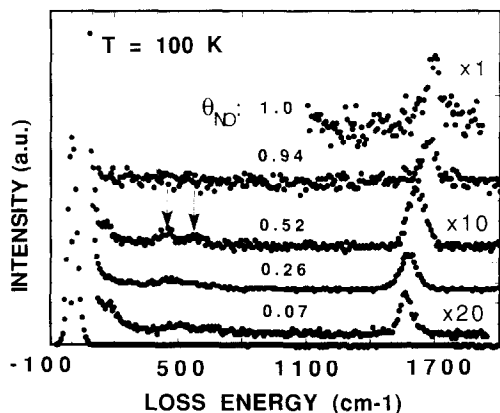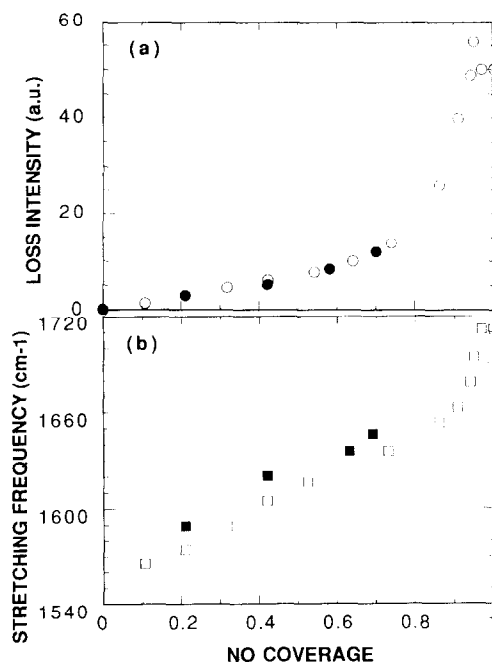Fig. 2. (a) Dependence of the loss intensity of the N–O stretching mode on the NO coverage, θ_{NO}, for NO adsorbed on Rh(110) at 100 K; (b) Variation of the N–O stretching frequency with NO coverage, θ_{NO}, on Rh(110) at 100 K. The filled symbols in (a) and (b) show the intensity and frequency variations for NO coadsorbing with a mixed layer of oxygen and nitrogen, deposited on Rh(110) by dissociation of $\theta_{NO} = 0.075$.

the 400–600 cm^{-1} region. At moderate coverages this broad feature develops into a doublet consisting of peaks located at 450 and 570 cm^{-1}. At high NO coverages these modes lose their intensity and can hardly be distinguished because of the enhanced background noise.

Fig. 2 presents the variations in the intensity, I_{N-O}, and frequency, ω_{N-O}, of the N–O stretch as a function of NO coverage on Rh(110) at 100 K. Initially, the intensity and peak frequency increase linearly with NO coverage up to $\theta_{NO} \sim 0.75$. Above this NO coverage both I_{N-O} and ω_{N-O} display an accelerated increase. At NO coverages very close to saturation the absorption intensity decreases, whereas the stretching frequency levels off at 1710 cm^{-1}. The same figure also shows the data on intensity and frequency changes versus coverage for NO adsorbing on a surface modified by O and N. O and N were

Fig. 1. HREEL spectra for increasing NO coverages on Rh(110) after adsorption at 100 K.

introduced onto the surface in a preliminary experiment by dissociation of $\theta_{NO} = 0.075$. It is evident that, excepting the slightly higher ω_{N-O} values (by ~ 20 cm^{-1}), the NO loss intensity and adsorption configuration are hardly affected by the presence of O and N up to $\theta_{NO} \sim 0.8$.

3.2. Dissociation of NO overlayers at elevated temperatures

The dissociation of NO, adsorbed molecularly on the surface at 100 K, is studied for the NO coverage range $0 < \theta_{NO} < 0.3$ when the NO coverage does not influence the dissociation rate. At higher coverages the NO dissociation becomes dependent on the availability of surface sites for the dissociation products. As has already been described in a number of papers, above a certain NO coverage partial desorption of NO should precede the dissociation process [20–26]. Thus a complex dependence of the dissociation process on NO coverage exists because the activation energy for NO desorption is higher than the activation energy for dissociation on Rh surfaces [20–26].

At $\theta_{NO} < 0.3$, NO dissociation on Rh(110) occurs upon heating at temperatures above 170 K. The amount of dissociated NO for the same initial NO coverage depends on the temperature and the duration of heating. Taking HREEL spectra after different heating times at a chosen temperature, followed by rapid cooling down to 100 K, provides valuable information about the dissociation process.

When the surface temperature is increased above 170 K substantial changes in the HREEL spectra occur. These changes are illustrated in figs. 3 and 4. Figs. 3a and 3b show two sets of HREEL spectra (for two initial NO coverages) acquired after different annealing times at 204 K. The annealing at this temperature causes a rather fast decrease in I_{N-O}. This is accompanied by an intensity gain of the peaks at 440 and 570 cm^{-1} and the emergence of new losses at ~ 350, 780 and 880 cm^{-1}. Since for the chosen NO coverage range no NO desorption occurs, the changes in the HREEL spectra are only due to temperature induced dissociation of NO. Figs. 4a–4c show the decrease of loss intensity and the concomitant frequency shift of the N–O band as a function of the annealing time at 204 K for three initial NO coverages. The data in figs. 3 and 4 provide the following useful information: (i) the completion of the NO dissociation at 204 K is coverage dependent, i.e., the fraction of undissociated NO increases with increasing initial NO coverage; (ii) the initial slope of the intensity versus time curves is proportional to the initial loss intensity; (iii) the increase in the amount of dissociation products causes an increase of the N–O stretching frequency of the remaining NO molecules. The ω_{N-O} values are by ~ 40 cm^{-1} higher when N(a) and
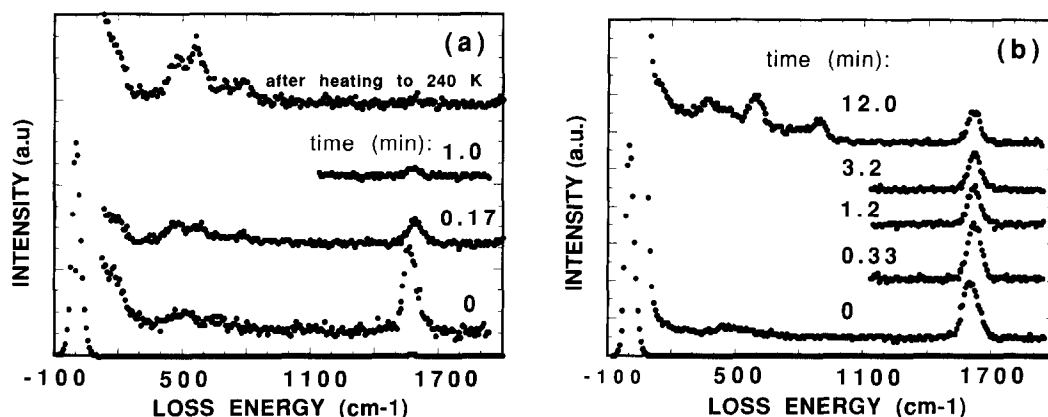

Fig. 3. HREEL spectra measured after increasing heating times at 204 K for NO layers adsorbed on Rh(110) at 100 K: (a) initial $\theta_{NO} = 0.075$; (b) initial $\theta_{NO} = 0.3$.
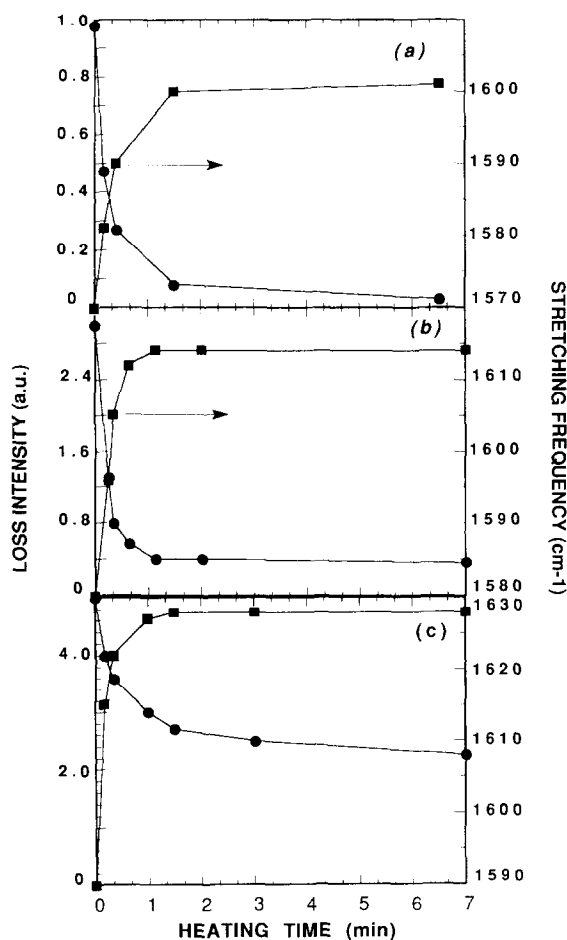
Fig. 4. Variations in the intensity and stretching frequency of the N–O stretch mode with increasing heating time at 204 K. The initial NO coverages, θ_{NO}, of NO adsorbed at 100 K on Rh(110) are: (a) 0.075; (b) 0.18; (c) 0.3.

Fig. 5. HREEL spectra measured after complete dissociation of NO for two initial coverages, θ_{NO}, of NO adsorbed at 100 K on Rh(110).

O(a) are present than those measured for the same NO coverage on a clean Rh(110) surface. For NO coverages less than 0.3 a further increase in temperature up to ~ 240 K leads to complete dissociation of NO and only the low frequency features remain visible in the HREEL spectra.

Fig. 5 displays the low energy region of HREEL spectra measured after complete dissociation of NO (adsorbed at 100 K) by rising the surface temperature to 300 K. It is obvious that the number of loss features which emerge upon NO dissociation and also their absorption intensities and frequencies depend on the absolute amount of dissociated NO. When the initial NO coverage is less than ~ 0.1 the main features after dissoci-
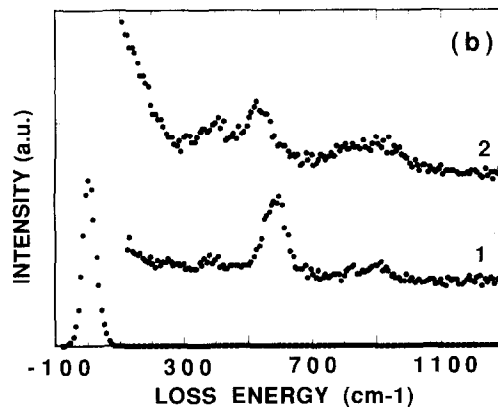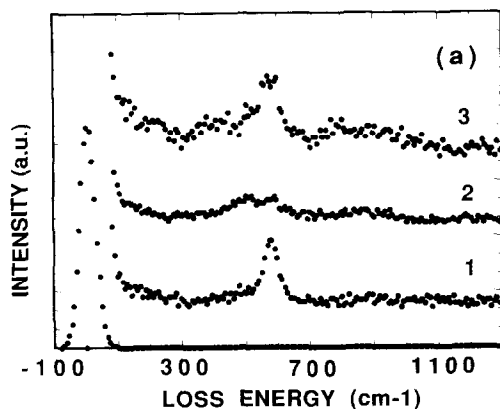

Fig. 6. HREEL spectra for increasing oxygen exposures on Rh(110) at adsorption temperatures: (a) 100 K; (b) 300 K. Spectrum 3 in (a) represents the changes in spectrum 2 (measured after oxygen adsorption at 100 K) induced by heating to 273 K.
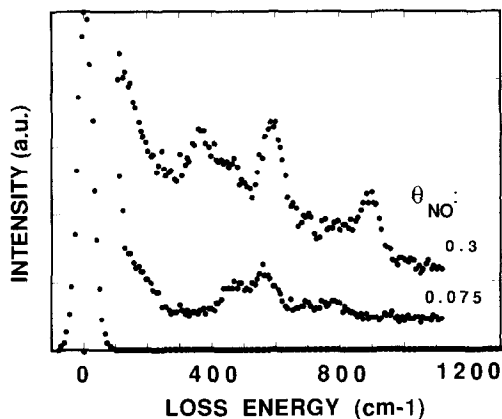
ation are at ~ 450 and 570 cm^{-1} with a weak broad shoulder in the 600–800 cm^{-1} range. When the initial NO coverages are higher, a peak at 350 cm^{-1} and a structure at ~ 900 cm^{-1} are observed as well.

In order to describe the origin of the features in the HREEL spectra which appear as a result of NO dissociation we carried out separate HREEL studies on nitrogen, oxygen and mixed nitrogen and oxygen adlayers on Rh(110).

Fig. 6 shows the HREEL spectra recorded after O$_2$ adsorption on Rh(110) at 100 and 300 K. It can be clearly seen that the oxygen vibrational spectrum depends substantially on the adsorption temperature and oxygen coverage. For oxygen adsorption at 100 K, the HREEL data (fig. 6a) show that: (i) low oxygen coverages are characterized by a vibrational mode in the 550–570 cm^{-1} range; (ii) higher oxygen coverages lead to three extra features at ~ 360, 500 and 850 cm^{-1}. The development of the HREEL spectrum at 300 K is presented in fig. 6b. It contains an intensive feature at 570 cm^{-1} at low oxygen coverages which is replaced by a feature at 500 cm^{-1} at higher coverages. A loss peak at 370 cm^{-1} and a broad poorly resolved doublet with components at ~ 800 and 900 cm^{-1} also appear at high coverages.

Spectrum 1 in fig. 7 presents the HREEL spectrum of a N layer deposited on Rh(110) after

Fig. 7. HREEL spectra of nitrogen deposited onto Rh(110) by dissociative adsorption of NH$_3$ (spectrum 1), after coadsorption of oxygen at 100 K (spectrum 2) and after heating the mixed layer to 300 K (spectrum 3).

dissociation of NH$_3$ and removal of hydrogen by temperature-induced desorption. The Rh–N vibration is characterized by a band at 415 cm^{-1}. Subsequent adsorption of oxygen (spectrum 2) at 100 K induces an extra loss at ~ 570 cm^{-1} and a shoulder at ~ 360 cm^{-1} and causes a slight blue-shift of the Rh–N stretch to 440 cm^{-1}. Heating of this mixed layer to 300 K causes the following changes in the intensities of the loss features: (i) the peak at 440 cm^{-1} due to the Rh–N stretch is strongly attenuated; (ii) the intensity of the 360 cm^{-1} peak increases and (iii) a shoulder at ~ 660 cm^{-1} and a peak at 850 cm^{-1} appear. The spectrum of the mixed N + O layer resembles that observed after NO dissociation (see fig. 5).

4. Discussion

4.1. NO bonding configuration on Rh(110) at 100 K

The NO stretching frequencies observed in the present study cannot be described unambiguously on the basis of the vibrational data for NO adsorption on other single-crystal metal surfaces [1–20,22,34] or considering the frequencies measured for transition metal nitrosyl complexes [36–39]. According to the frequency assignments for transition metal nitrosyls, the·N–O stretching mode measured in the present study is within the range of on-top bent NO: 1525–1700 cm^{-1} [6,17,36] . The two low-frequency bands can be assigned to the Rh–N stretching (440 cm^{-1}) [22] and Rh–N–O bending (570 cm^{-1}) [39] modes. In the framework of a predominantly bent configuration up to medium coverages the observed significant increase in the intensity and frequency of the N–O modes and the strong suppression of the low-frequency modes at high NO coverages can be explained as being due to the conversion from a bent to a linear bonding geometry. However, the following information raises questions about the consistency of this interpretation of the vibrational data: (i) the measurements of the intensity of the elastic and loss peaks as a function
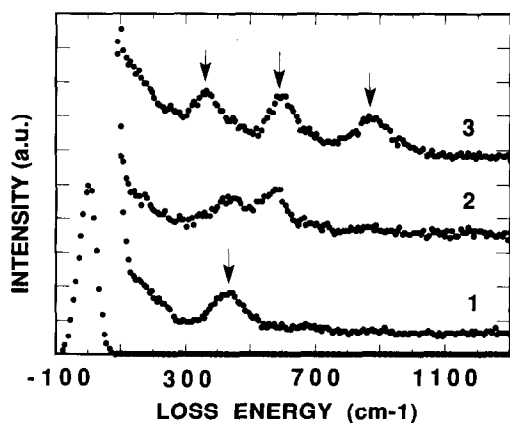
of the deviation angle from the specular direction showed a behaviour dominated by the cross section changes, i.e., they do not provide evidence for the existence of off-normally bound NO molecules on Rh(110) at 100 K; (ii) the low-energy vibrational region resembles that observed for small amounts of oxygen and nitrogen coadsorbed on Rh(110); and (iii) the N–O stretching frequency of 1710 cm^{-1}, measured at close to saturation NO coverages seems a bit low for a dense layer of on-top NO with a linear geometry.

Another alternative explanation of the NO loss spectra on Rh(110) is a single linear adsorption geometry into bridge sites, similar to the case of NO adsorption on Rh(111) [13]. In this case, in order to explain the low-energy region of the loss spectra, it is postulated that a tiny amount of NO undergoes dissociation (most probably on defects) even at 100 K. This will result in the appearance of Rh–N (440 cm^{-1}) and Rh–O (570 cm^{-1}) bands. The HREEL data for nitrogen, oxygen and mixed nitrogen and oxygen adsorption systems, obtained in the present study either by separate nitrogen and/or oxygen deposition or after NO dissociation at elevated temperatures, show that: (i) the Rh–N stretching mode of adsorbed nitrogen atoms appears at 415 cm^{-1} and suffers a blue shift by ~ 30 cm^{-1} in the presence of oxygen; (ii) low coverages of oxygen adsorbed at 100 K are characterized by a Rh–O stretching frequency at 570 cm^{-1} hardly affected by the presence of coadsorbed nitrogen; (iii) mixed N + O layers obtained after decomposition of small amounts of NO (θ_{NO} ~ 0.075) upon heating to 200 K, results in two bands at ~ 460 and 570 cm^{-1}, the intensity of the latter being strongly damped by the presence of undissociated NO. Similar strong suppression of the oxygen loss peak induced by coadsorbed NO molecules was also observed on Rh(111) [13] and Ru(001) [19]. A survey of the available data on adsorption and dissociation of NO on transition metal surfaces shows that NO dissociation can occur at temperatures ranging from 80 to 140 K for low NO coverages on Ag(111) [34], W(100), [32], Mo(100) [33] and Rh(100) [20]. Since the activity of the more open Rh(110) surface should be higher than that of the Rh(100) surface it is probable that a

small amount of NO dissociates on defect sites of a Rh(110) surface even at temperatures as low as 100 K.

Accepting the second model for explaining the HREEL spectra of NO on Rh(110) a linear bridge-bonding NO configuration should be justified. Comparison with the available vibrational data for NO/transition metal adsorption shows that the energy region of the N–O band on Rh(110) is closest to that (1580–1680 cm^{-1}) reported for linear bridge-bonded NO on Rh(100) [20]. The NO stretching frequency range measured in the present study exceeds that found by Villarrubia and Ho [20] only at NO coverages close to saturation (see fig. 2). This may well be due to the fact that at high coverages the NO molecules can be forced to occupy sites influenced by the introduced tiny amounts of dissociation products. The results obtained in separate studies of NO adsorption on Rh(110) precovered with a mixed N + O overlayer and the frequency shift observed in the course of heating experiments (see figs. 2 and 4) support this explanation. It should be emphasized that a blue-shift induced by electronegative coadsorbates is a common phenomenon [13,19,40–45] in cases when the metal/$2\pi^*$ backbonding component contributes mainly to the molecular adsorption bond. The following contributions could account for the blue-shift: (i) dipole effects due to electrostatic (direct or via the substrate) interactions between the coadsorbates; (ii) chemical effects due to competition for "backdonation" electrons, (iii) changes in the adsorption site or bonding geometry, and (iv) an increase of the local concentration provided the interactions in the mixed overlayer force the coadsorbed molecules to form separate islands.

Usually, the metal–NO frequencies reported for bridge bonded NO are in the 300–400 cm^{-1} range [5,6,10–13,34]. For NO on Rh(111) the Rh–NO vibration induces a very weak feature at 360 cm^{-1} which can be distinguished only at high NO coverages. The lack of a similar feature in our HREEL spectra may well be due to a lower dynamical dipole of NO on the Rh(110) surface. The absence of the Me–NO mode was reported for the bridging NO on Ru(0001) [1,2].

4.2. NO dissociation and HREEL spectra of NO dissociation products

The HREELS data in the present study provide evidence that a substantial fraction of NO undergoes dissociation on Rh(110) at temperatures higher than 170 K. The ratio of the initial slopes of the loss intensity versus annealing time plots, displayed in figs. 4a–4c, is $1:2.1:3.3$. Let us assume that for the NO coverage range under consideration in figs. 4a–4c the initial dissociation rate, r_0, obeys the simple relationship: $r_0 = k_0 \theta_{NO}(1 - \theta_{NO})$ where k_0 remains constant. This leads us to the ratio $1:2.1:3.1$ for the initial dissociation rates at $\theta_{NO} = 0.075$, 0.18 and 0.3, respectively. This result is in very good agreement with the values obtained from the initial slopes of the intensity versus time in figs. 4a–4c for the same θ_{NO}. This means that within the low NO coverage range concerned in the present study, the initial dissociation rate exhibits first-order coverage dependence. This conclusion is correct because, as shown in fig. 2a, in the low NO coverage range the loss intensities vary linearly with NO coverage and are not influenced by the presence of small amounts of dissociation products. We have not attempted to make quantitative conclusions about the overall NO dissociation kinetics on the basis of the HREEL data because the presence of larger amounts of dissociation product might affect the loss intensity in an unpredictable direction. The loss intensity versus annealing time data show that at temperatures lower than 240 K the fraction of undissociated NO increases with increasing NO coverage and with decreasing annealing temperature. This observation can be explained by a picture where the nearest accessible sites for NO dissociation are already blocked by the dissociation products. Thus, further dissociation requires diffusion to favourable surface sites, which obviously becomes an activated process in the presence of dissociation products.

The introduction of O and N adatoms in the course of NO dissociation also causes a blue-shift in the N–O stretching mode of the order of 40 cm^{-1} compared to the same NO coverage on a clean surface. This shift is larger (by ~ 20 cm^{-1}) than the shift measured for NO post-adsorbed on a surface containing a mixed O + N layer (fig. 2) though the amount of O and N is almost the same. This difference is due to the fact that when NO is adsorbing on a modified surface it occupies preferentially sites that are least affected by the preadsorbed O and N. Consequently, at low NO coverages, effects such as weak next-nearest neighbour interactions [45] and an increase of the local NO surface density mainly contribute to the observed relatively small blue shift. Similar weak effects on the NO bridging configuration at low NO and O coverages were reported for other systems [13,17,19,44,45]. The picture is quite different when the NO molecules remain on the surface as an undissociated fraction. In this case, the O and N modifiers introduced in the course of dissociation, may be located quite near to the nondissociated molecules. Provided the diffusion of the latter is impeded then they would bare a shorter-range influence causing the larger blue shift. The factors that contribute to the blue-shift have already been discussed in the previous section 4.1.

Finally, let us attempt to describe the origin of the loss features that appear in the frequency region below 1000 cm^{-1} after dissociation of NO on Rh(110). The present loss spectra are substantially different from those observed after similar NO dissociation experiments on Rh(111) [13], where only a prominent loss feature at 530 cm^{-1}, assigned to adsorbed oxygen atoms, remains after NO dissociation. Although conclusive identification of the induced loss features requires more in depth studies, the comparison of the loss spectra obtained after separate oxygen and/or nitrogen adsorption with that observed after NO dissociation shows that, excepting the feature at 440 cm^{-1} (which can be safely assigned to the Rh–N stretching mode), the other loss features can be related to oxygen.

A multi-loss peak spectrum for an one component adsorption system is indicative for the presence of a great variety of adsorption states and possible formation new phases. One of the most thorough studies of the system O/Ni(110) [46,47] has shown successive oxygen chemisorption, oxygen-induced reconstruction and formation of an

oxide phase. The different oxygen states allow for different vibrational modes, e.g., oxygen adsorbed on unreconstructed surface areas is characterized by a dipole active mode at 500 cm^{-1}, oxygen adsorbed on a reconstructed surface by modes at 280, 390 and 800 cm^{-1} and NiO growth (in smaller or larger islands) by two modes at $\sim$ 450 and 550 cm^{-1} and overtones at higher energy. Another example is the O/Pd(111) system where the Pd–O stretching mode of chemisorbed oxygen is at $\sim$ 500 cm^{-1} and the initial formation of PdO is characterized by new vibrational modes at 275, 675 and 750 cm^{-1} [48]. Commonly, the intermediate states of formation of bulk oxides are characterized by losses within the 700–1000 cm^{-1} range [40,46–48]. These frequencies, which are relatively high compared to those characteristic of chemisorbed oxygen and bulk oxide, are related to oxygen penetrating below the first metal layer [40]. Oxygen brought onto the Ni(111) surface by decomposition of NO was reported to be even more effective than oxygen alone in producing a high frequency feature at $\sim$ 950 cm^{-1} associated with an intermediate oxidation state of Ni [40].

The activity of Rh single-crystal surfaces varies with the crystallographic orientation. The closed-packed Rh(111) surface is the most resistant to oxidation and only a single mode at 530 cm^{-1}, characteristic of a chemisorption state, was observed after adsorption of oxygen or dissociation of NO [13]. Oxygen adsorption on stepped Rh surfaces leads to an extra feature at $\sim$ 750 cm^{-1} after annealing and reconstruction at high oxygen coverages [49]. The LEED and HREEL studies of oxygen adsorption on Rh(100) have shown a variety of surface structures and an appearance of new loss features at 465, 515, $\sim$ 700 and 990 cm^{-1} at high oxygen coverages and elevated temperature. These features rise at the expense of the vibrational peak of the chemisorbed oxygen at 415 cm^{-1} [50]. Recently, dynamical LEED analyses of the (2 × 2)p2gg structure observed at an oxygen coverage of one-half monolayer have shown that even at temperatures as low as 130 K oxygen can induce a weak reconstruction of the Rh(100) surface [51]. Baird et al. reported the appearance of a (2 × 1)p1g1 LEED pattern and two O 1s XPS peaks at 529 and 531 eV for oxygen

adsorption on Rh(110) at 300 K [26]. A similar O 1s XPS spectrum and the same LEED pattern were observed after NO dissociation. The double-peak structure in the O 1s region is indicative of the existence of at least two oxygen states on the surface.

Since the formation of an oxide phase by penetration of oxygen through the surface is easier for more open surface structures [52], the Rh(110) surface is expected to be less resistant to reconstruction and oxide formation than Rh(111) and Rh(100) [53]. Thus, the peaks observed in the loss spectra presented in figs. 5 and 6 can be assigned to different states of oxidation involving initial chemisorption, possible reconstruction and growth of oxide islands. In the case of NO dissociation, nitrogen atoms also are introduced onto the surface. It has been found that for some surfaces, e.g., Ni(100) [53] the nitrogen-induced reconstruction is even stronger than that induced by oxygen. Thus, it can be supposed that nitrogen also will influence the Rh(110) structure and will contribute to the eventual surface reconstruction and oxide formation.

5. Summary

NO adsorption on Rh(110) at 100 K and subsequent decomposition in the temperature range 170–250 K have been studied using HREEL spectroscopy. The main findings in this investigation can be summarized as follows:

(1) There is one adsorption state of NO at 100 K, assigned to bridge-bonded NO species. Depending on the NO coverage this state is characterized by N–O stretching frequencies from 1560 to 1710 cm^{-1}.

(2) For NO coverages less than 0.3 of the saturation coverage at 100 K measurable decomposition of adsorbed NO starts at temperatures above 170 K although that the HREELS data give evidence for dissociation of tiny amounts of NO (probably on defect sites) even at 100 K. The fraction of dissociated molecules depends on temperature and heating time and is larger for lower initial NO coverages. The HREEL measurements of the intensity of N–O mode provide

evidence that the initial dissociation rate is first order in NO coverage for the NO coverage range under consideration.

(3) The dissociation products (O and N), introduced on the surface in the course of NO decomposition, hinder further decomposition of NO and cause an increase of the N–O stretching frequency of the undissociated NO molecules. Depending on the initial NO coverage a critical temperature is required for completion of dissociation. This effect is related to a diffusion barrier that should be surmounted by the remaining NO molecules in looking for favourable sites for dissociation. A possible explanation of the increased N–O stretching frequency is that the undissociated NO molecules are squeezed among the dissociation products. The latter exert electrostatic and chemical effects typical for the electronegative modifiers.

(4) Existence of one adsorption state of nitrogen and several adsorption states of oxygen (which might involve reconstruction and/or different oxidation states) is suggested in order to explain the HREEL spectra measured after complete dissociation of different amounts of NO on Rh(110).

Acknowledgements

References

[1] P.A. Thiel, W.H. Weinberg and J.T. Yates, Jr., Chem. Phys. Lett. 67 (1979) 403.
[2] G.E. Thomas and W.H. Weinberg, Phys. Rev. Lett. 41 (1978) 1181.
[3] P. Feulner, S. Kulkarni and D. Menzel, Surf. Sci. 99 (1980) 489.
[4] U. Schwalke and H.W. Weinberg, J. Vac. Sci. Technol. A 5 (1987) 459.
[5] J.C.L. Cornish and N. Avery, Surf. Sci. 235 (1990) 209.
[6] G. Pirug, H.P. Bonzel, H. Hopster and H. Ibach, J. Chem. Phys. 71 (1979) 593.
[7] M. Kiskinova, G. Pirug and H.P. Bonzel, Surf. Sci. 136 (1984) 285.
[8] J.L. Gland and B. Sexton, Surf. Sci. 94 (1980) 355.
[9] B.E. Hayden, Surf. Sci. 131 (1983) 419.
[10] H. Ibach and S. Lehwald, Surf. Sci. 76 (1978) 1.
[11] C. Nyberg and P. Uvdal, Surf. Sci. 204 (1988) 517.
[12] M. Bertolo and K. Jacobi, Surf. Sci. 226 (1990) 207.
[13] T.W. Root, G.B. Fisher and L.D. Schmidt, J. Chem. Phys. 85 (1986) 4679, 4687.
[14] S. Jorgensen, N.D.S. Canning and R.J. Madix, Surf. Sci. 179 (1987) 322.
[15] P. Ho and J.M. White, Surf. Sci. 137 (1984) 103.
[16] S. Lehwald, J.T. Yates, Jr. and H. Ibach, Proc. Forth Int. Conf. Solid Surfaces, Cannes, Le Vide, Les Couches Minces 201 (1980) p.221.
[17] G. Odorfer, R. Jaeger, G. Illing, H. Kuhlenbeck and H.-J. Freund, Surf. Sci. 233 (1990) 44, and references therein.
[18] H.-P. Steinrück, C. Schneider, P.A. Heimann, T. Pache, E. Umbach and D. Menzel, Surf. Sci. 208 (1989) 136.
[19] H. Conrad, R. Scala, W. Stenzel and R. Unwin, Surf. Sci. 145 (1984) 1.
[20] J.S. Villarrubia and W. Ho, J. Chem. Phys. 87 (1987) 750.
[21] D.G. Castner and G.A. Somorjai, Surf. Sci. 83 (1979) 60.
[22] C.-T. Kao, G.S. Blackman, M.A. Van Hove, G.A. Somorjai and C.-M. Chan, Surf. Sci. 224 (1989) 77.
[23] P.A. Thiel, J.T. Yates, Jr. and W.H. Weinberg, Surf. Sci. 82 (1979) 22.
[24] T.W. Root, L.D. Schmidt and G.B. Fisher, Surf. Sci. 134 (1983) 30, 150 (1985) 173.
[25] L.A. DeLouise and N. Winograd, Surf. Sci. 159 (1985) 199.
[26] R.J. Baird, R.C. Ku and P. Wynblatt, Surf. Sci. 97 (1980) 346.
[27] H.-D. Schmick and H.-W. Wassmuth, Surf. Sci. 123 (1982) 471.
[28] H. Conrad, G. Ertl, J. Kuppers and E.E. Latta, Surf. Sci. 65 (1977) 235.
[29] J. Kanski and T.N. Rhodin, Surf. Sci. 65 (1977) 63.
[30] D.E. Ibbotson, T.S. Wittig and W.H. Weinberg, Surf. Sci. 110 (1981) 294.
[31] S. Tatarenko, M. Alnot and R. Ducros, Surf. Sci. 163 (1985) 249.
[32] T. Kioka, M. Yokota, H. Miki, S. Sugai and K. Kawasaki, Surf. Sci. 216 (1987) 409.
[33] J.P. Fulmer and W.T. Tysoe, Surf. Sci. 233 (1990) 35.
[34] S.-K. So, R. Franchy and W. Ho, J. Chem. Phys. 91 (1989) 5701.
[35] K.C. Taylor, in: Catalysis and Automobile Pollution Control, Eds. A. Crucq and A. Frennet (Elsevier, Amsterdam, 1987) p. 97.
[36] F.A. Cotton and G. Wilkinson, Advanced Inorganic Chemistry (Wiley, New York, 1972) p. 713.
[37] J. Muller and S. Schmidt, J. Organomet. Chem. 97 (1975) C54.
[38] JANAF, Thermochemical Tables, 2nd ed., Natl. Stand. Ref. Data Ser., NBS No 37 (1971).

[39] E. Miki, K. Mizumachi, T. Ishimori and H. Onuko, Bull. Chem. Soc. Jpn. 41 (1968) 1835; 46 (1973) 3779.

[40] H. Ibach and D.L. Mills, Electron Energy Loss Spectroscopy and Surface Vibrations (Academic Press, New York, 1982).

[41] F.M. Hoffmann, Surf. Sci. Rep. 3 (1983) 107.

[42] Y.J. Chabal, Surf. Sci. Rep. 8 (1988) 21.

[43] M. Kiskinova, Surf. Sci. Rep. 8 (1988) 359.

[44] B.E. Hayden, K. Kretzschmar and A.M. Bradshaw, Surf. Sci. 125 (1983) 366.

[45] J.G. Chen, W. Erley and H. Ibach, Surf. Sci. 224 (1989) 215.

[46] S. Masuda, M. Nishijima, J. Sakisaka and M. Onchi, Phys. Rev. B (1982) 863.

[47] B. Voigtlander, S. Lehwald and H. Ibach, Surf. Sci. 225 (1990) 162.

[48] B. Banse and B. Koel, Surf. Sci. 232 (1990) 275.

[49] D. Belton, G.B. Fischer and G. DiMaggio, Surf. Sci. 233 (1990) 12.

[50] L.H. Dubois, J. Chem. Phys. 77 (1982) 5228.

[51] W. Oed, B. Dötsch, L. Hammer, K. Heinz and K. Müller, Surf. Sci. 207 (1988) 55.

[52] G.A. Somorjai and M.A. Van Hove, Progr. Surf. Sci. 30 (1989) 201.

[53] G.L. Kellogg, J. Catal. 92 (1985) 167, J. Vac. Sci. Technol. A 4 (1986) 1419.

[54] W. Daum, S. Lehwald and H. Ibach, Surf. Sci. 178 (1986) 528.